

Feline injection site sarcoma: computed-tomographic density and assessment of tumor dimensions by different methods¹

Karen Maciel Zardo^{2*}, Lucas Petri Damiani³, Julia Maria Matera⁴
and Ana Carolina B.C. Fonseca-Pinto⁵

ABSTRACT- Zardo K.M., Damiani L.P., Matera J.M. & Fonseca-Pinto A.C.B.C. 2017. **Feline injection site sarcoma: computed-tomographic density and assessment of tumor dimensions by different methods.** *Pesquisa Veterinária Brasileira* 37(10):1113-1118. Departamento de Cirurgia, Faculdade de Medicina Veterinária e Zootecnia, Universidade de São Paulo, Cidade Universitária, Avenida Prof. Orlando Marques de Paiva 87, São Paulo, SP 05508-270, Brazil. E-mail: kmzardo@gmail.com

Feline injection site sarcoma is a malignant neoplasm with digitiform projections into muscular planes that are ill recognized during physical examination and may compromise tumor margin demarcation. This study compared tumoral size of 32 cats measured by different methods, and evaluated the CT density of 10 tumoral tissues (Hounsfield unit) based on histograms. Tumor axes were measured by physical examination and CT images. Larger craniocaudal axis measurements were obtained following multiplanar reconstruction of pre- and post-contrast CT images ($p=0.049$ and $p=0.041$ respectively); dorsoventral axis measurements taken from post-contrast CT images were also larger ($p=0.010$). Tumor volume estimates increased following contrast-enhancement. Histograms tended to produce two peaks: one in the fat and another in the soft tissue attenuation range. Multiplanar reconstructed post-contrast CT images provided clearer definition of tumor margins and more judicious determination of tumor size. A tendency of common FISS attenuation profile could be described.

INDEX TERMS: Feline injection-site sarcoma, tumoral density, computed tomographic, tumoral dimension.

RESUMO.- [Sarcoma de aplicação felino: avaliação da densidade tomográfica e das dimensões tumorais por diferentes métodos.] O sarcoma de aplicação felino (SAF) é uma neoplasia maligna que geralmente apresenta projeções digitiformes para planos musculares adjacentes, dificilmente reconhecidos ao exame físico, o que pode comprometer a real identificação das suas margens. Este estudo comparou as dimensões tumorais de 32 SAFs mensurados por diferentes métodos (exame físico e por imagens de to-

mografia computadorizada) e avaliou a densidade tomográfica em unidades Hounsfield de 10 dessas neoplasias, com base em histogramas. As medidas no eixo craniocaudal foram maiores quando obtidas após reconstrução multiplanar de imagens tomográficas, tanto na fase pré como após administração de meio de contraste ($p=0,049$ e $p=0,041$, respectivamente). As medições tomográficas no eixo dorsoventral obtidas na fase pós-contraste também foram maiores, quando comparadas com as imagens pré-contraste ($p=0,010$). Estimativas do volume tumoral foram maiores após a fase contrastada. Os histogramas das densidades tumorais tenderam a produzir dois picos: o primeiro no intervalo de valores de densidade gordura e o segundo no intervalo correspondente a tecidos moles. As imagens tomográficas pós-contraste com reconstrução multiplanar demarcaram com mais clareza as margens do tumor e definiram de forma mais criteriosa o seu tamanho. Uma tendência de perfil de atenuação comum para o SAF pôde ser descrita com esse estudo.

TERMOS DE INDEXAÇÃO: Sarcoma de aplicação felino, densidade tumoral, tomografia computadorizada, dimensões tumorais.

¹ Received on October 13, 2015.

Accepted for publication on September 4, 2016.

² Departamento de Cirurgia, Faculdade de Medicina Veterinária e Zootecnia (FMVZ), Universidade de São Paulo (USP), Av. Professor Orlando Marques de Paiva 87, São Paulo, SP 05508-270, Brazil. *Corresponding author: kmzardo@gmail.com

³ Departamento de Estatística, Instituto de Matemática e Estatística, USP, Rua do Matão 1010, São Paulo, SP 05508-090.

⁴ Departamento de Cirurgia, FMVZ-USP, Av. Professor Orlando Marques de Paiva 87, São Paulo, SP 05508-270. E-mail: materajm@usp.br

⁵ Departamento de Cirurgia, FMVZ-USP, Av. Professor Orlando Marques de Paiva 87, São Paulo, SP 05508-270. E-mail: anacarol@usp.br

INTRODUCTION

Feline injection site sarcoma (FISS) is a malignant, locally invasive subcutaneous neoplasm with high recurrence rates (McEntee & Page 2001, Martano et al. 2011). The condition was first described in the 1990s when clinicians speculated that severe acute vaccine-associated inflammatory reactions progressed to sarcoma. Feline injection site sarcoma has attracted increasing attention in the scientific community ever since (Martano et al. 2011, Srivastav et al. 2012, Sparkes 2013). However, despite several research efforts over the last decades, the etiology of FISS remains undetermined (Woodward 2011, Sparkes 2013). Feline injection site sarcomas tend to form digitiform projections that invade deeper muscular planes (Samii 2007, Martano et al. 2011, Carneiro 2012, Travetti et al. 2013) and are seldom recognized on physical examination; these projections prevent clear definition of surgical margins and adequate demarcation of radiotherapy fields (VAFSTF 2005). The highly invasive nature of even small-sized FISSs calls for multidisciplinary diagnostic approaches. Cross-sectional imaging modalities such as computed tomography (CT) and magnetic resonance imaging (MRI) are recommended for effective treatment planning (VAFSTF 2005, North & Banks 2009, Martano et al. 2011).

Comparative studies of FISS volume based on CT images and clinical findings (McEntee & Samii 2000, McEntee & Page 2001, Carneiro 2006, Di Giancamillo et al. 2011, Carneiro 2012, Travetti et al. 2013, Zardo et al. 2013) have failed to reach a consensus. While CT yielded larger mean tumor volume estimates than physical examination in most articles, (McEntee & Samii 2000, McEntee & Page 2001, Carneiro 2006, Zardo et al. 2013) no significant differences were reported in others (Di Giancamillo et al. 2011, Carneiro 2012). Significantly larger tumor volume estimates from post-contrast compared to pre-contrast CT images have also been reported (McEntee & Samii 2000), but were not confirmed in a later study (Zardo et al. 2013). Although studies investigating FISS CT density are scarce, mean values fall within the soft tissue attenuation range have been reported (Carneiro 2012, Zardo et al. 2013).

This study was designed to: (1) compare the size of FISS lesions estimated by physical examination with corresponding CT measurements, and tumor volume estimated from pre- and post-contrast CT images; (2) determine density values and describe common attenuation patterns of FISS lesions based on histograms obtained from pre- and post-contrast CT images. Our hypotheses were that measurements made from post-contrast CT images would provide more judicious estimations of tumor size and volume, and that multiplanar reconstruction (MPR) would enable clearer definition of tumor margins; furthermore tumor histograms would provide additional data for CT characterization of FISS lesions.

MATERIALS AND METHODS

The information contained in this article was extracted from a Master's thesis by the first author (Zardo 2014). All animal procedures in this study were approved by the Animal Ethics Committee of the Faculty of Veterinary Medicine and Animal Science

of the University of São Paulo (protocol number 2705/2013); all owners consented to the inclusion of their cats in the study.

This study comprised cats of variable gender, body weight and age. Patient selection was based on the presence of solid masses at injection sites and cytological and/or histological diagnosis of FISS (nonrecurrent and recurrent neoplasms).

The prospective phase included cats referred to the veterinary hospital in 2013 and submitted to physical examination and CT. Tumor size estimation was based on physical measurements of tumor length (craniocaudal axis, CC), width (laterolateral axis, LL) and height (dorsoventral axis, DV). Measurements (cm) were made using a caliper by a single veterinary radiologist (KMZ). CT images were acquired using a helical single-slice CT scanner (Xpress - GX Spiral; Toshiba America Medical Systems) with 120kVp, 150mA, tube rotation time 1.0s., matrix dimensions 512 x 512 and 3 mm slice thickness at 1.5 mm reconstruction intervals. Contrast-enhanced scans were performed 90 seconds after intravenous *bolus* injection of iohexol (Omnipaque® 300, GE Healthcare).

The retrospective phase of the study was based on medical records and tomographic imaging of cats scanned at the veterinary hospital between 2005 and 2012. Tomographic imaging records were analyzed by veterinary radiologist (KMZ) blinded to previous CT reports. Tumor size data (CC, LL and DV axes) made during physical examination using a caliper were extracted from medical records. CT images were acquired using either a helical single-slice CT scanner (Xpress - GX Spiral, Toshiba America Medical Systems, 4 cases) or an axial CT scanner (CT-Max 640, GE Healthcare 27 cases). Tomographic images (120kVp, 150mA, tube rotation time 1.0s, matrix dimensions 512x512) were acquired with slice thickness and increments/reconstruction intervals between 2.5 and 10mm according to tumor size. Contrast-enhanced scans were performed immediately after intravenous *bolus* injection of iohexol (Omnipaque® 300, GE Healthcare, 2 cases) or meglumine amidotrizoate and sodium-ionic dimmer (Urografina 292®, Berlimed SA, 25 cases).

Contrast media were administered at 450mg I/kg doses. Images were reconstructed using soft tissue and bone algorithms. Transverse CT slices were planned to fully encompass the neoplastic area detected on topograms and extended approximately 3cm beyond perceptible margins, which is the minimal recommended surgical margins (Martano et al. 2011), with cats in sternal recumbency. All digital tomographic images were stored in the PACS (Synapse 4.0, Fujifilm Medical System, Valhalla, New York) and exported into a DICOM viewer (OsiriX Imaging Software 5.8.1 32 bit, Pixmeo).

Tomographic measurements of tumor axes were first taken from pre- and post-contrast transverse CT images, then following MPR of DICOM images in the OsiriX system. Measurements (cm) were standardized as follows. **Without MPR:** The longest LL and DV axes were subjectively identified in tomographic slices; measurements were then made using the "Length ROI" tool. The cursor was aligned according to the obliquity of each tumor. The CC axis was calculated by multiplication of the number of slices where the tumor was visible by the increment/reconstruction interval. **With MPR:** The reference line for sagittal reconstruction was placed parallel to the tumor axis in the transverse viewing window and the longest DV axis subjectively identified. The procedure was repeated in the dorsal reconstruction window for subjective identification of the longest CC and LL axes. Measurements were then made using the "Length ROI" tool. Tumor volume (cm³) was estimated from pre- and post-contrast CT images using the standard OsiriX procedure with the "Brush ROI" tool.

There was not an internal command available in Osirix for the automatic generation of volume histogram when the study was performed. For this, regions of interest (ROIs) demarcating neoplastic lesions were defined in all CT slices where neoplasms

could be recognized. The export ROIs plugin was then employed to create XML (eXtensible Markup Language) files containing the attenuation values (HU) of each tumor voxel. Files were imported into R® statistical software (R Development Core Team) for histogram generation (-300 HU and +300 HU cutoff points).

Statistical analyses were made using software (R®, R Development Core Team). The level of significance was set at 5%. Continuous variables were described using measures of position (mean, median, minimum and maximum values) and scale (standard deviation - SD). The non-parametric Mann-Whitney test was used to compare continuous variables with two characteristics (the non-parametric test was used due to the small sample size). Repeated measurements (measurements taken from the same cat by different methods) were compared using the paired Mann-Whitney (2 characteristics) or the Friedman (3 or more characteristics) test. The paired comparisons were made just with CT images in DICOM format (n=10 cases).

RESULTS

Thirty-two cats were selected in this study. Selected cats were aged between 2 and 15 years (mean age, 10.06±3.63

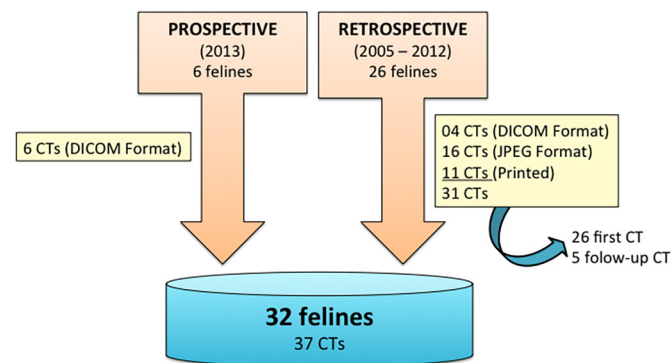


Fig.1. Scheme showing the composition of the prospective and retrospective groups of this study with respect to CT exams.

years) and weighed between 3.4 and 8.8 kg (mean body weight, 5.19±1.2 kg). There were evaluated 16 female and 16 male cats; 5 Siamese and 27 mixed breed cats. A total of 37 CT scans (31 retrospective and 6 prospective) were analyzed. Five out of 37 CT scans corresponded to follow-up assessments. Four patients (retrospective study) were not submitted to contrast-enhanced CT due to chronic renal failure. CT images included in the retrospective study were stored in DICOM or JPEG file format, or printed on film (4, 16 and 11 images respectively). All images acquired in the prospective study were stored in DICOM file format (Fig.1).

Most tumors had poorly defined margins (23/37, 62%), with clearer margin demarcation in post-contrast compared to pre-contrast CT images. A CT scout view of wide area coverage (about 3cm beyond perceptible tumor margins) was not enough to fully encompass the neoplastic area in 15 out of 37 FISS cases studied (40.5%) and mildly thickened muscular tissues were left out.

Tumors size according to axis and method of measurement is given in Table 1. Physical measurements of CC and DV axes differed significantly from corresponding pre- and post-contrast CT measurements (Table 2). This values were submitted to multiple comparisons and physical measurements tended to yield smaller tumor length estimates (CC axis) compared to pre- and post-contrast CT (p<0.001, Table 3). Conversely, post-contrast CT tended to yield larger tumor height estimates (DV axis) compared to pre-contrast CT (p=0.048, Table 3) and physical examination (p=0.041, Table 3). Tumor length (CC axis) was the most discrepant measurement between methods (p<0.001, Table 3). Pre and post-contrast CT measurements performed before and after MPR were compared by Paired Mann-Whitney test (Table 4). Multiplanar reconstruction yielded larger estimates of tumor length (CC axis) on pre and post-contrast images

Table 1. Descriptive statistics of tumor size according to axis and method of measurement

Axis	Method of measurement	N	Minimum (cm)	Maximum (cm)	Mean (cm)	SD (cm)	Median (cm)
Craniocaudal	Physical examination	36	0.50	12.00	4.38	2.79	4.00
	Pre-contrast CT	37	2.30	13.00	7.10	2.98	6.90
	Pre-contrast MPR CT	10	2.28	13.93	7.44	2.99	7.28
	Post-contrast CT	33	2.30	13.00	7.23	3.20	7.00
	Post-contrast MPR CT	10	2.37	15.09	7.80	3.27	7.38
Laterolateral	Physical examination	36	0.50	12.00	3.08	2.28	2.80
	Pre-contrast CT	37	0.80	9.13	3.04	2.06	2.82
	Pre-contrast MPR CT	10	1.06	8.87	3.28	2.63	2.23
	Post-contrast CT	33	0.79	9.17	3.20	2.14	2.78
	Post-contrast MPR CT	10	0.70	6.20	2.80	1.88	2.32
Dorsoventral	Physical examination	36	0.50	12.00	4.69	2.83	5.00
	Pre-contrast CT	37	0.80	8.71	5.34	1.92	5.45
	Pre-contrast MPR CT	10	4.14	8.01	6.19	1.46	6.47
	Post-contrast CT	33	0.80	9.15	5.56	2.10	5.72
	Post-contrast MPR CT	10	3.00	8.51	6.37	1.81	6.71

Table 2. comparisons of physical, pre- and post-contrast measurements (cm) of tumor size

Axis	Physical examination			Pre-contrast CT			Post-contrast CT			P Value
	Median	1st quartile	3rd quartile	Median	1st quartile	3rd quartile	Median	1st quartile	3rd quartile	
CC	4	2.075	5.25	6.9	4.8	9	7	4.65	9.6	0.001
LL	2.8	1.5	4	2.82	1.5	3.9	2.78	1.52	4.02	0.297
DV	5	2.375	6	5.45	4.08	6.96	5.72	4.44	7.05	0.022

Friedman Test (n=2).

Table 3. Multiple comparisons of significant Friedman Tests given in Table 2

Multiple Comparisons	P value for CC	P value for DV
Pre-contrast CT x Physical examination	<0.001	0.998
Post-contrast CT x Physical examination	<0.001	0.041
Post-contrast CT x Pre-contrast CT	0.421	0.048

Table 4. Comparison of tumor axes (cm) measured on pre-contrast and pre-contrast MPR CT images

Axis	Pre-contrast CT			Pre-contrast MPR CT			P value
	Median	1st quartile	3rd quartile	Median	1st quartile	3rd quartile	
CC	6.90	4.80	9.00	7.28	6.16	8.26	0.049
LL	2.82	1.50	3.90	2.23	1.55	4.67	0.193
DV	5.45	4.08	6.96	6.47	4.93	7.37	0.084

Paired Mann-Whitney Test (n=10).

Table 5. Comparisons of tumor axes (cm) measured on post-contrast and post-contrast MPR CT images

Axis	Post-contrast CT			Post-contrast MPR CT			P value
	Median	1st quartile	3rd quartile	Median	1st quartile	3rd quartile	
CC	7.00	4.65	9.60	7.38	6.27	9.05	0.014
LL	2.78	1.52	4.02	2.32	1.52	3.45	0.554
DV	5.72	4.44	7.05	6.71	4.99	7.81	0.010

Paired Mann-Whitney Test (n=10).

Table 6. Descriptive statistics of tumor volume measured on pre- and post-contrast CT images of 10 cats (DICOM images)

Variable	Confidence interval for means (95%)						
	Minimum (cm ³)	Maximum (cm ³)	Mean (cm ³)	SD (cm ³)	Median (cm ³)	Lower (cm ³)	Upper (cm ³)
Pre-contrast volume	1.56	184	53.2	62.42	19.1	8.54	97.9
Post-contrast volume	1.17	187	54.4	63.13	20.1	9.23	99.5
Difference (post-contrast, pre-contrast)	-0.39	3	1.2a	0.99	1.3	0.48	1.9

P value = 0.004 (Paired Mann-Whitney Test).

Table 7. Descriptive statistics of FISS attenuation values (Hounsfield Unit) according to contrast phase

Variable	Factor	N	Minimum	Maximum	Mean	Standard	P value*
Contrast phase	Post	10	-59.0	73.1	20.6	38.6	0,002
	Pre	10	-77.5	55.1	-0.4	37.2	
Total		20	-77,5	73.1	10.1	38.4	

*Paired Mann-Whitney test.

(Table 4, p=0.049; Table 5, p=0.014 respectively) and height (DV axis) on post-contrast images (Table 5, p=0.010). There was no statistical difference between the LL axis measured in this sample. Tumor volume estimates based on DICOM CT image files of 10 cats are given in Table 6. Tumor volume tended to be consistently larger when determined from post-contrast compared to pre-contrast CT images (mean difference 1.2cm³, p=0.004; ρ de Pearson = 0.999).

Tumor CT density was expressed as pre- and post-contrast attenuation values (Hounsfield Unit - HU) (Table 7). Significantly higher mean HU values were observed on post-contrast scans in all cases (p=0.002). These values were grouped according to recurrence or nonrecurrence of neoplasms, and higher mean pre- and post-contrast attenuation values were documented in recurrent (23.29 and 47.66 HU

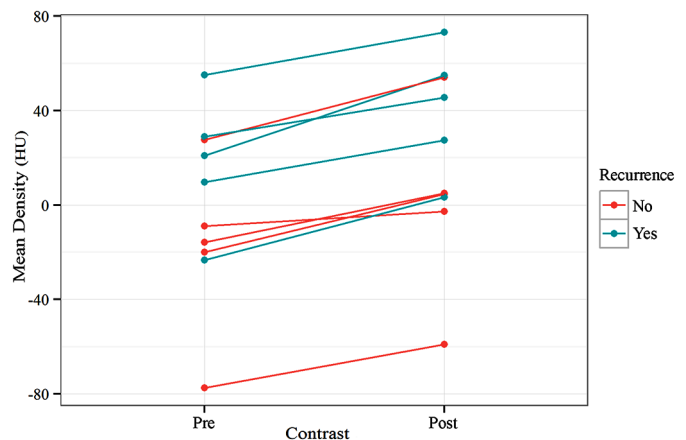


Fig.2. Mean tumor density (HU - Hounsfield unit) in pre- and post-contrast phases. Increased attenuation (HU) in the post-contrast phase can be seen in recurrent and non-recurrent neoplasms.

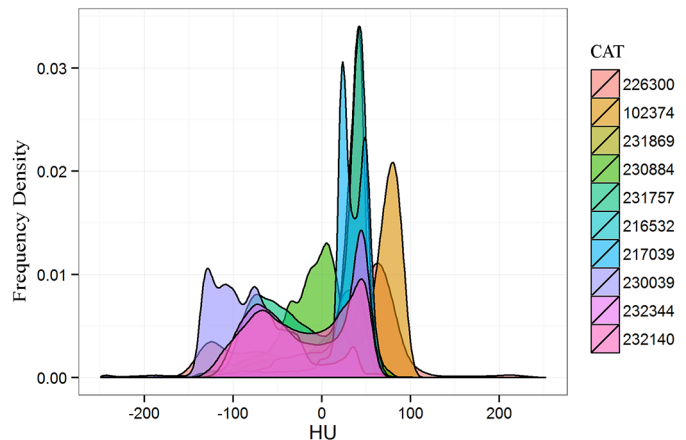


Fig.3. Histogram showing the frequency of pre-contrast CT attenuation values in 10 FISSs.

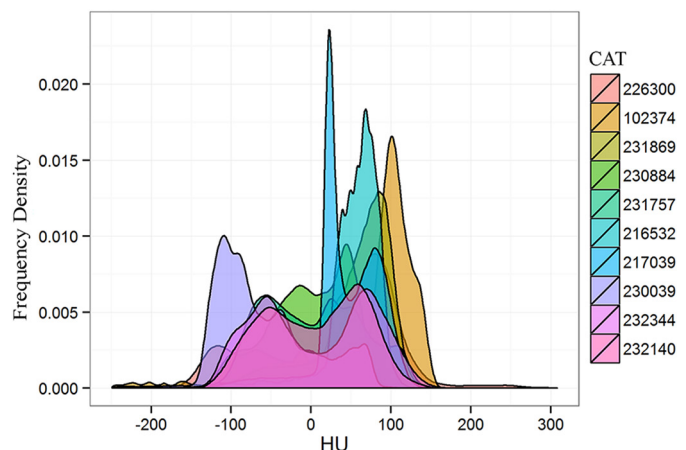


Fig.4. Histogram showing the frequency of post-contrast CT attenuation values in 10 FISSs.

respectively) compared to nonrecurrent neoplasms (-14.5 and 4.04 HU respectively); however, differences were not statistically significant (p>0.05, Mann-Whitney test). Mean tumor density (HU - Hounsfield unit) in pre- and post-contrast phases are displayed in Fig.2. Histograms revealed curves with two distinct peaks (Fig.3 and Fig.4): a lower,

broader peak in the negative attenuation range (fat density; -120 to -80 HU) and a higher, narrower peak in the positive attenuation range (soft tissue density, 40 to 60 HU). Contrast enhancement shifted curves slightly to the right (Fig.4), particularly the second peak, which also became broader and lower. Relatively stable pre- and post-contrast attenuation values in the 0-20 HU range (fluid density) were also observed.

DISCUSSION

In accordance with previous reports (Carneiro 2006, 2012, Sparkes 2013), cats affected with FISS in this study were generally adults and overweight, with no gender or breed predisposition.

The highly invasive computed tomographic appearance of even small FISS lesions support the significance of CT for accurate determination of tumor extension prior to treatment (McEntee & Page 2001). As in canine mast cell tumors (Lorigados et al. 2013), CT was a more accurate method of measurement than physical examination in this study, particularly in cases where neoplasms projected into surrounding tissues. Moreover, CT recognition of blurring of fat planes, that may represent highly inflamed and vascularized peritumoral tissues or neoplastic infiltration of the panniculus (Webb 2000), that are seldom detected on physical examination plays an important role in effective surgical planning (Travetti et al. 2013). Tumors in this study appeared larger on CT than physical examination, particularly when measurements were taken from post-contrast MPR CT images. Largest discrepancies documented in CC axis measurements between methods may have reflected the inclusion of digitiform projections in tomographic estimates of tumor size, easily recognized on CT scans but not on physical examination. Results of the current study support recent CT data (Travetti et al. 2013) suggesting that FISS masses have longer CC and DV axes, in this order. Better understanding of FISS growth patterns and behavior is required to clarify the significance of these findings.

Multiplanar reconstruction yielded larger CC (pre- and post-contrast tomograms) and DV (post-contrast tomograms) axis length estimates in this trial. Three-dimensional CT measurement of neoplastic lesions, particularly those with ill-defined margins, may be challenging (Travetti et al. 2013). Contrast enhancement is recommended for accurate tumor margin demarcation (Samii 2007) and proved helpful for tumor size determination in this study. Multiplanar reconstruction was also vital for accurate measurement of FISS lesions in the sample considered. Tumor length has been shown to be more easily measured in reconstructed CT images (Kinns et al. 2001). Better understanding of peritumoral anatomy in the sagittal and dorsal planes (Kinns et al. 2001) further support the significance of MPR in the assessment of neoplastic lesions. Good quality reconstructed CT images were obtained using 3 mm slices and 1.5 mm increments in this study, despite poorer resolution compared to transverse images. Thinner submillimeter slices can improve MPR and increase image spatial resolution in the sagittal and dorsal planes, particularly when multidetector CT scanners are used (Kinns et al. 2001).

Topograms with wide area coverage was not enough to fully encompass the neoplastic area in some FISS cases studied and mildly thickened muscular tissues were left out. Referring clinicians should be aware of this fact when planning for surgery. Extension of the topogram 5 cm beyond palpable tumor margins, which is the maximal recommended surgical margins (Martano et al. 2011), is therefore indicated in cases of FISS. Also, larger numbers of tomographic slices should be considered upon recognition of suspected areas.

Highly discrepant mean FISS volumes have been reported elsewhere (McEntee & Samii 2000, Carneiro 2006, 2012, Travetti et al. 2013). Accordingly, tumor volume estimates were highly variable in this study and may have reflected differences in time spans from onset of clinical manifestations to search for veterinary advice by cat owners. Comparative data on mean FISS volume determined by different measurement methods are somewhat conflicting. While most studies documented larger mean tumor volume based on CT images compared to physical measurements (McEntee & Samii 2000, McEntee & Page 2001, Carneiro 2006), trials involving 33 (Carneiro 2012) and 200 (Di Giancamillo et al. 2011) FISS cases failed to report significant differences between methods. In the aforementioned studies, volume calculation was either based on common formulas used for geometry figures (e.g. ellipsoid) or not specified. Traditional geometric formulas are designed for regular-shaped figures and may not apply to irregularly shaped tumors such as those in this sample. Hence, tumor volume estimates based on tomographic and physical examination were not compared in this study and only tumor volume estimated by software (i.e. accounting for tumor margin irregularity) from pre- and post-contrast CT images were considered. As previously reported (McEntee & Samii 2000), consistently larger tumor volumes were documented in post- compared to pre-contrast CT scans in this study (mean difference, 1.2 cm³). These findings support the value of contrast-enhanced CT in determination of tumor volume and accurate tumor margin demarcation.

Besides aiding in surgical planning, unidimensional and volumetric measurements of neoplasms are advocated for evaluation of clinical responses to chemo and radiotherapy. Despite limitations (e.g. increase in tumor size and volume in response to inflammation and positive response of necrotic areas to treatment), therapeutic response assessment is still largely based on measurements of tumor size, particularly in studies comparing new protocols and well-established methods of treatment (Stacchiotti et al. 2009, Lorigados et al. 2013). Magnetic resonance imaging is the gold standard for determination of size and extension of soft tissue sarcomas in humans (Knapp et al. 2005). Future studies including MRI-based measurements of FISS lesions are warranted.

Quantification of attenuation in HU is helpful for organ or tissue characterization and identification of potential abnormalities (Lorigados et al. 2013). Although data on HU values of FISS are scarce, mean FISS attenuation values within the soft tissue range have been reported (Carneiro 2012, Zardo et al. 2013). Lower mean values were docu-

mented in this study; however, standard deviations were high given the prevailing heterogeneous density of FISS lesions. Highly discrepant minimum and maximum attenuation values within the same neoplasm have also been observed in canine mast cell tumor studies (Lorigados et al. 2013).

Higher mean HU in the post- compared to pre-contrast phase was documented in all cases in this sample (Fig.2). Most post-contrast image acquisitions were delayed; therefore, increased HU may have reflected low contrast washout, consistent with tumor malignancy (Slattery et al. 2006). Specific dynamic CT perfusion studies are required to investigate this hypothesis.

It was thought that non-recurrent neoplasms would have lower attenuation values compared to recurrent neoplasms due to surgical resection of tumor-associated adipose tissue components. Low statistical power (small sample size) precluded detection of such differences despite higher mean pre- and post-contrast attenuation values in recurrent compared to non-recurrent neoplasms. Future studies with larger sample sizes are therefore warranted.

Patterns on the histograms in this study may have reflected the combined effects of increased density in response to the presence of contrast medium in the tumor parenchyma and resulting heterogeneous contrast enhancement. Areas with higher and lower blood vessel density were highlighted in the post-contrast phase; wider attenuation value ranges may have resulted, although with greater frequency variation compared to the pre-contrast phase. Constant values in the 0 to 20 HU range may have reflected areas of liquefactive intratumoral necrosis.

In cases where the time of image acquisition was not standardized (4 cases, retrospective study), curves with similar shape but slightly skewed to the left or right might have been expected. However, minor differences in image acquisition time between retrospective and prospectively analyzed tomograms had no significant impact on histogram curve shape.

FISS attenuation patterns may vary according to lesion site, histological type and degree of malignancy. Larger sample sizes, comparisons with other types of neoplasms and application of modern multi-detector technology for multiphase dynamic studies and tumor perfusion pattern analysis should be considered in future studies.

CONCLUSIONS

Based on the results of this study, MPR post-contrast CT images provide clearer definition of tumor margins and contributes to judicious determination of tumor size.

Histograms of tumor attenuation values provided a general overview of FISS tissue composition and a tendency of common FISS attenuation profile was demonstrated in this study.

Acknowledgements.- The authors would like to express their thanks to National Council for Scientific and Technological Development - CNPq, process n° 301986 / 2013-4, and Dr. Carolina Scarpa Carneiro from the Faculty of Veterinary Medicine and Animal Science, University of São Paulo, for the medical records employed in the retrospective phase of this study.

REFERENCES

- Carneiro C.S. 2006. Clinical study of the effect doxorubicin in the feline injection-site sarcoma. MSc Dissertation, Faculty of Veterinary Medicine and Animal Science, University of São Paulo, São Paulo, SP.
- Carneiro C.S. 2012. Characterization of patients with feline injection-site sarcoma as body condition score and as to the origin of its formation and their microenvironment. PhD Thesis, Faculty of Veterinary Medicine and Animal Science, University of São Paulo, São Paulo, SP.
- Di Giancamillo M., Travetti O., Stefanello D., Zecconi A., Ravasio G. & Grieco V. 2011. The relationship between tumor volume and local invasiveness in feline injection-site sarcoma: a retrospective CT study on 200 cases. *Vet. Radiol. Ultrasound* 52(2):215-236.
- Kinns J., Malinowski R., McEvoy F., Schwarz T. & Ziwngenberger A. 2001. Special softwares applications, p.70-71. In: Schwarz T. & Saunders J. (Eds), *Veterinary Computed Tomography*. Wiley-Blackwell, West Sussex, UK.
- Knapp E.L., Kransdorf M.J. & Letson G.D. 2005. Diagnostic imaging update: soft tissue sarcomas. *Cancer Control J.* 12(1):22-26.
- Lorigados C.A.B., Matera J.M., Coppi A.A., MacEdo T.C., Ladd F.V.L., Sousa V.A.F. & Pinto A.C.B.C.F. 2013. Tomografia computadorizada de mastocitomas em cães: avaliação pré- e pós-tratamento quimioterápico. *Pesq. Vet. Bras.* 33(11):1349-1356.
- Martano M., Morello E. & Buracco P. 2011. Feline injection-site sarcoma: past, present and future perspectives. *Vet. J.* 188(2):136-141.
- McEntee M.C. & Page R.L. 2001. Feline vaccine-associated sarcomas. *J. Vet. Intern. Med.* 15(3):176-182.
- McEntee M.C. & Samii V.F. 2000. The utility of contrast enhanced tomography in feline vaccine associated sarcomas: 35 cases. *Vet. Radiol. Ultrasound* 41(6):575.
- North S. & Banks T. 2009. Sarcomas of the skin and subcutaneous tissue: feline sarcomas, p.173-182. In: North S. & Banks T. (Eds), *Small Animal Oncology: an introduction*. Saunders Elsevier, Philadelphia.
- Samii V.F. 2007. The thoracic wall, p.519-524. In: Thrall D.E. (Ed.), *Textbook of Veterinary Diagnostic Radiology*. 5th ed. Saunders Elsevier, St Louis.
- Slattery J.M., Blake M.A., Kalra M.K., Misdraji J., Sweenwy A.T., Copeland P.M., Muelles P.R. & Boland G.W. 2006. Adrenocortical carcinoma: contrast washout characteristics on CT. *Am. J. Roentgenol.* 187(1):W21-24.
- Sparkes A. 2013. Current thinking on feline injection site sarcomas. 2nd chance info. Available from <<http://www.2ndchance.info/fibrosarcoma-Sparkes2013.pdf>> Last accessed Sept. 3, 2015.
- Srivastav A., Kass P.H., McGill L.D., Farver T.B. & Kent M.S. 2012. Comparative vaccine-specific and other injectable-specific risks of injection-site sarcomas in cats. *J. Am. Vet. Med. Assoc.* 241(5):595-602.
- Stacchiotti S., Collini P., Messina A., Morosi C., Barisella M. & Bertulli R. 2009. High grade soft tissue sarcomas: tumor response assessment: pilot study to assess the correlation between radiology and pathologic response by using RECIST and Choi criteria. *Radiology* 25(2):447-456.
- Travetti O., Di Giancamillo M., Stefanello D., Ferrari R., Giuduce C., Grieco V. & Saunders J.H. 2013. Computed tomography characteristics of fibrosarcoma: a histological subtype of feline injection-site sarcoma. *J. Feline Med. Surg.* 15(6):488-493.
- VAFSTF 2005. Vaccine-Associated Feline Sarcoma Task Force, roundtable discussion; the current understanding and management of vaccine-associated sarcomas in cats. *J. Am. Vet. Med. Assoc.* 226(11):1821-1842.
- Zardo K.M., Fonseca-Pinto A.C.B.C., Carneiro C.S., Matera J.M., Sendyk-Grunkraut A. & Lorigados C.B. 2013. Aspectos tomográficos do sarcoma de aplicação felino. *Arch. Vet. Sci.* 18(2):34.
- Zardo K.M. 2014. Ultrasonographic and tomographic characterization of feline injection site sarcoma. MSc Dissertation, Faculty of Veterinary Medicine and Animal Science, University of São Paulo, São Paulo, SDP.
- Webb W.R. 2000. Mediastino: anormalidades linfonodais e massas tumorais, p.34-60. In: Webb W.R., Brant W.E. & Helms C.A. (Eds), *Fundamentos de Tomografia Computadorizada do Corpo*. 2ª ed. Guanabara Kooogan, Rio de Janeiro.
- Woodward K.N. 2011. Origins of Injection-Site Sarcomas in Cats, the possible role of chronic inflammation: a review. *ISRN Vet Sci.* 2011(210982):1-16.